# Stainless steel membrane roof

Autor(en): **Kato, Ben / Nakamichi, Takashi / Saeki, Eiichiro**

Objekttyp: **Article**

Zeitschrift: **IABSE reports = Rapports AIPC = IVBH Berichte**

Band (Jahr): **49 (1986)**

PDF erstellt am: **22.07.2024**

Persistenter Link: https://doi.org/10.5169/seals-38303

# Stainless Steel Membrane Roof

## Membranes en acier inoxydable pour toitures

## Nichtrostende Stahlmembrane für Bedachungen

**Ben KATO**
Prof. of Struct. Eng.
University of Tokyo
Tokyo, Japan

**Takashi NAKAMICHI**
Techn. Adm. Bureau
Nippon Steel Corporation
Tokyo, Japan

**Eiichiro SAEKI**
Struct. Engineer
Nippon Steel Corporation
Tokyo, Japan

Ben Kato, born 1929, received his degree of Dr. Eng. from the University of Tokyo. Through the continuing service as lecturer, associate professor at the University of Tokyo, Ben Kato, now occupies the chair of steel structures and welding engineering.

Takashi Nakamichi, born in 1938, received his Bachelor's degree from Kyushu Univ. Since 1962 he has been engaged in building design and construction and now is engaged in the development and engineering of architectural materials and structures.

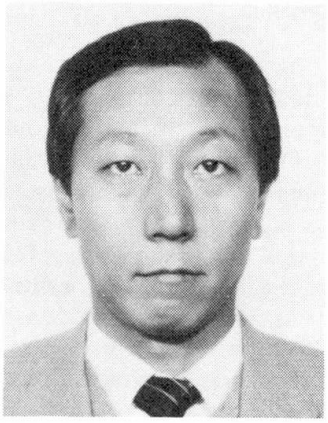

Eiichiro Saeki, born 1951, received his M. Eng. from Tokyo Institute of Technology and M.Sc. from Northwestern Univ., USA. Since 1976 he has been engaged in the design and construction of buildings, now involved in the research and development of special structures.

**SUMMARY**

The design procedure for stainless steel membrane roofs is described with reference to the recently completed double-membrane roof project. Especially the behaviour of the contraction joints is discussed taking into account the stress condition of the cold-forming process.

**RÉSUMÉ**

La procédure de dimensionnement d'une toiture utilisant des membranes d'acier inoxydable est décrite en se référant à un projet de couverture utilisant des doubles membranes d'acier inoxydable dont la construction fut réalisée tout récemment. On examine en particulier le comportement des assemblages de contraction en tenant compte de l'état de contrainte lors du processus de profilage à froid.

**ZUSAMMENFASSUNG**

Das Konstruktionsverfahren einer nichtrostenden Stahlmembran-Bedachung ist hierin beschrieben, wobei auf das Projekt eines Doppelmembrandaches Bezug genommen wird, das vor kurzem fertiggestellt wurde. Das Verhalten der Kontraktionsverbindungen wurde eingehend behandelt, wobei der Spannungszustand infolge Kaltverformung berücksichtigt wurde.

## 1.INTRODUCTION

In the period from the latter half of the 1960s to the early years of the 1970s, extensive studies were conducted on metallic membrane roofs in Canada. As a result of such studies, it was found that chrome-nickel stainless steel is most suitable as a material for permanent type membrane roofs. Moreover, the basic behavior of such membrane roofs under pressures and loads was elucidated. The suitability of stainless steel as a material for membrane roofs is due to its excellent characteristics, such as high strength to withstand large stresses with small thickness, corrosion resistance high enough to assure long-term durability, toughness high enough to resist pitting, tearing, etc., and excellent weldability to facilitate fabrication and assembly. For the practical application of stainless steel membrane to large-scale structure, however, the following three conditions must be satisfied:

-(1)It must be possible to assemble the roof on a flat surface.
-(2)The completed roof should be maintained in a spherical shape by air pressure.
-(3)The completed roof should be formed into a concave shape at deflation.

The condition (1) is essential for practical construction of membrane roofs. If the condition (2) is not satisfied, the characteristic of the shell cannot be produced. If the condition (3) is not met and the internal pressure becomes insufficient after completion (deflation), buckling or other troubles may be caused, resulting in damage to the segments. Sinoski's system introduced below is a metallic membrane roof which satisfies the three conditions shown above by the use of contraction joints. This paper describes the design procedure of stainless steel membrane roof, mainly membrane stresses and contraction joints referring to the Health Promotion Center at Nippon Steel's Muroran Works which was the first project completed using the stainless steel double membrane roof (hereinafter referred to as the "Muroran Project").

## 2.OUTLINE OF STAINLESS STEEL MEMBRANE ROOF

### 2.1 Structural element

Basically, the membrane roof is constructed by assembling and welding stainless steel sheets (of about 1.5mm in thickness for a span of 100m) into a very large sheet. The roof thus constructed is supported by air pressure from below. More specifically, this roof consists of the following members as shown in Figs. 1 and 2.
Compression ring (a): Member to support the tension applied to the segment
Trapezoidal segment (b): Segment are cut from stainless steel sheet and are welded at the plant and transported to the site.
Center segment (c): Same as segment (b)
Contraction joints (d and f): These joints are formed by pressing at the plant.
Closure joint (e): Polyurethane sheet or a material having the flexibility and durability equivalent to those of polyurethane

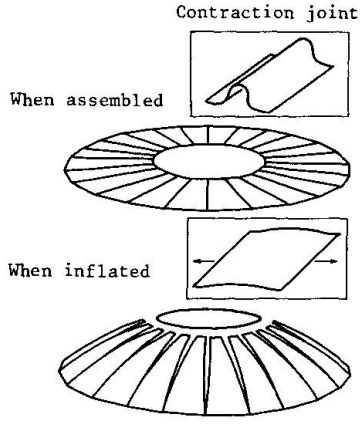


Fig. 1. System of stainless steel membrane roof

Basically, the segments are made of SUS304 and the contraction joints, SUS301 LHT (JIS). The membrane consists of six members (a) to (f) as described above. All members are joined mainly by welding. Spring members called "contraction joints" which can follow the expansion and contraction of the gap between the segments are used to ensure that the segments arranged on a flat surface can be formed into a spherical shape when the membrane is inflated (see Fig. 1). The roof can be inflated into a proper, stable dome by adjusting the spring characteristics, the amount of contraction and the arrangement of the contraction joints as appropriate.

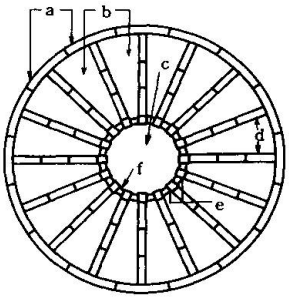


Fig. 2. Members of stainless steel membrane roof

## 3.DESIGN PROCEDURE

The flow chart for design of stainless steel membrane roofs is shown in Fig. 3. "Shape analysis" means the shape design of dome to be formed by inflation. In this design, the stable shape is determined in consideration of plan. "Structural analysis" means the analysis of membrane stress and compression ring stress which is undertaken using the above-mentioned shape. The details of this analysis are described in the following sub-chapter. The design of contraction joint is divided into two stages. In the first stage, the cross-sectional shape is designed to determine the arrangement and the amount of contraction of contraction joints which are necessary for developing the required dome shape. In the second stage, the spring characteristics of the contraction joint is analyzed in order to confirm that the specified dome shape can be developed when the membrane stresses calculated by structural analysis are applied, and to check the safety for the stresses to be caused in the contraction joints. (The details of this analysis are described in Chapter 3.)

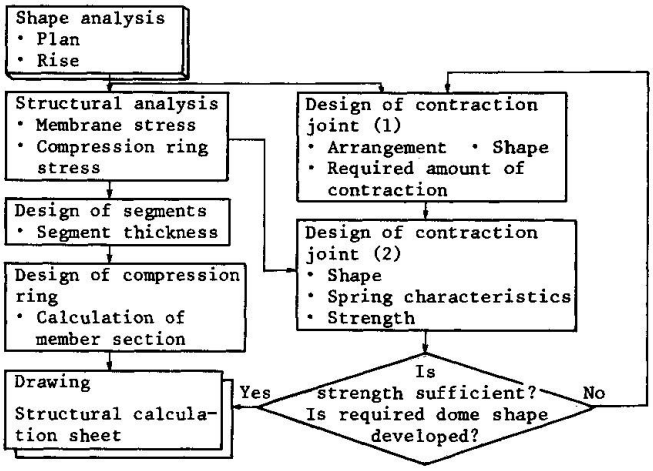


Fig. 3 Flow chart for design

### 3.1 Method for analysis of membrane stresses and compression ring stresses

The membrane and compression ring stresses are analyzed together according to the finite element method. The program and elements to be used for this analysis are shown below. In stress analysis, the shape obtained by fully extending the contraction joints is taken as the initial shape (it is assumed that the membrane is uniform and free from ondulations) and the stresses caused by internal pressures and other external forces are analyzed according to the small displacement theory. [A comparison of the stresses calculated by the small displacement theory with those obtained by the analysis in which the geometrical non-linearity is taken into account shows that the latter stresses are about 90% of the former stresses for this type of shape (in case where the internal pressure is 1.47kN/$m^2$).]

Program used: MARC
Elements used:
Segment: Three-dimensional thin-wall shell element
Compression ring: Three-dimensional beam element
As the two elements shown above have the same degree of freedom of node and boundary compatibility, they can be analyzed together.

## 3.2 Example of analysis of membrane stresses

### 3.2.1 Analytic model

An analytic model was assumed for the Muroran Project. This model is of such a shape, consisting of parts of sphere and cylinder with 30m in long side, 24m in short side and 1.1m in rise. The one-fourth model and element diagram for F.E.M. are shown in Fig. 4. The boundary conditions are such that the lines A and B are symmetrical and the nodes marked by ● which are the supporting points are free in the X and Y directions but constrained in the Z direction.

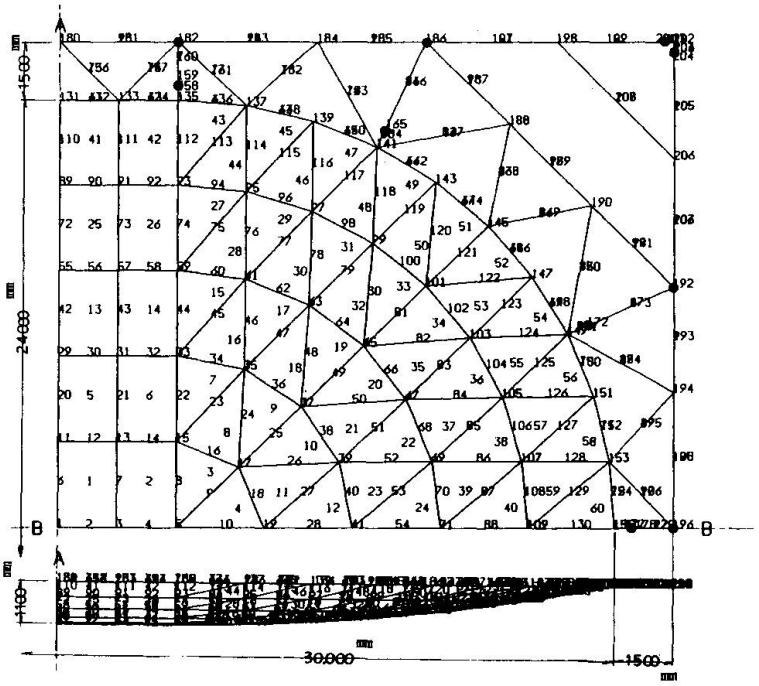


Fig. 4. Analytic model

### 3.2.2 Material constants

The material constants are as shown in Table 1.

Table 1 Material constants

| | Stainless steel | SS41 |
|---|---|---|
| Young's modulus | 19,306 kN/cm$^2$ | 20,580 kN/cm$^2$ |
| Poisson's ratio | 0.3 | 0.3 |

### 3.2.3 Loads

Two kinds of loads are assumed. One is the load in the normal direction which corresponds to internal pressure and wind load. The other is the load in the vertical direction which corresponds to dead load and snow load. As the example of analysis being introduced here is for the double membrane roof, the stiffness of the compression rings of this model was evaluated by proportionally distributing the stiffness of the compression rings of the single membrane analysis model according to the ratio of loads applied to the upper and lower membranes so that the deformation of the upper membrane edge agrees with that of the lower membrane edge.

### 3.2.4 Results of analysis

Examples of the results of analysis are shown in Figs. 5 and 6. Figs. 5 shows the Mieses stress intensity at the center of the cross section and Fig. 6 shows the displacement in the X and Y directions at a magnification of 100. As these results of analysis show, the distribution of membrane stresses differs considerably from that according to the spherical and/or cylindrical shell theory. Particularly, the stress concentration to be caused at the end of the cylindrical

shell is excessive. It is considered that this stress concentration results from the shape instability and the difference in boundary conditions. As this stress concentration is very sensitive to the dome shape and the rigidity of compression rings, it should be given special attention in future design. On the other hand, the stresses to be caused in the compression rings are considerably smaller than those to be caused in case where the reaction force at the membrane edge which is calculated according to the membrane theory is applied to the rings as an external force. This may be due to the effect of plane rigidity of the stainless steel membrane. Namely, it may be because the deformation of the rings in the Y direction is constrained by the plane rigidity.

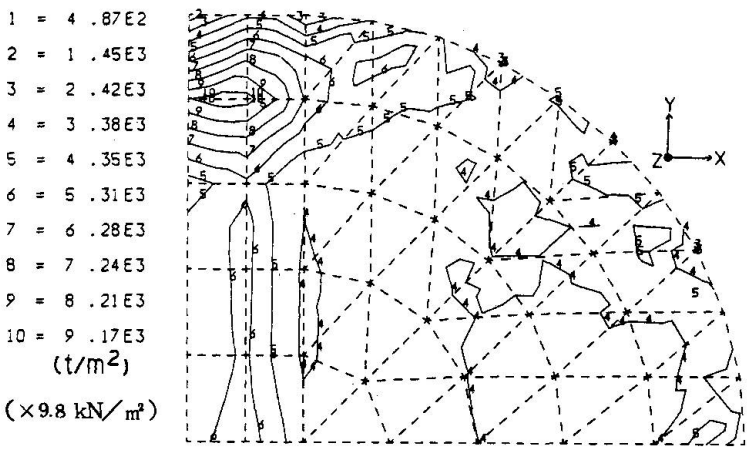


Fig. 5. Mieses stress

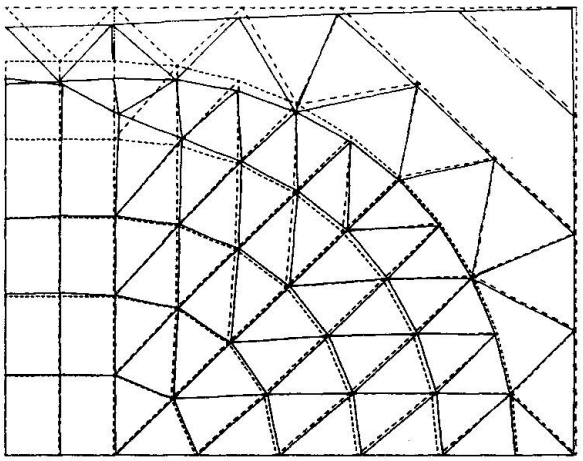

Fig. 6. Deformation diagram (x 100)

## 4.ANALYSIS OF THE MECHANICAL CHARACTERISTIC OF CONTRACTION JOINT

The contraction joint is the most important member of the stainless steel membrane roof. The designed curvature can be exactly produced and the development of undesirable stresses in the segments at the time of deflation can be prevented by arranging the contraction joints appropriately. The contraction joint is fabricated by cold-forming stainless steel sheet with high yield point. This joint expands nearly to a flat shape at the time of inflation but contracts nearly to its original shape at the time of deflation. In these cases, the residual stresses and strains developed within the contraction joint at the time of forming are changed in a complicated manner during the course of expansion and contraction. In Chapter 4, the structural safety of the contraction joint is studied by analyzing the behavior of this joint.

### 4.1 Analytic model of contraction joint

As shown in Fig. 7, the contraction joint can be expressed with the radius of curvature R and the angle $\theta$ as parameters. As the symmetry condition and the inflection point of bending moment are located close to the point Ⓠ, the analysis is conducted using the one-fourth model as shown in Fig. 8. In actual analysis, two radii of 20 and 30cm, $\theta$ of 30° and the sheet thickness of 0.15cm are used.

## 4.2 Analysis method

Analysis is conducted according to the finite element method in which material non-linearity (plasto-elasticity) and geometrical non-linearity (large deformation) are taken into consideration. For element division, the length between © and Ⓠ is divided into 100 elements and the cross section is divided into 20 layers. It is assumed that there is no stress change in each layer. The relation between the stress and strain is modelled as shown in Fig. 10 on the basis of the results of material test as shown in Fig. 9.

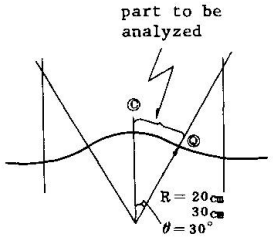


Fig. 7. Analytic model

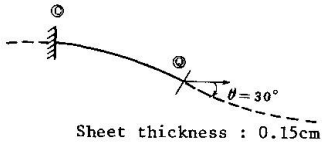


Fig. 8. Analytic model (1/4)

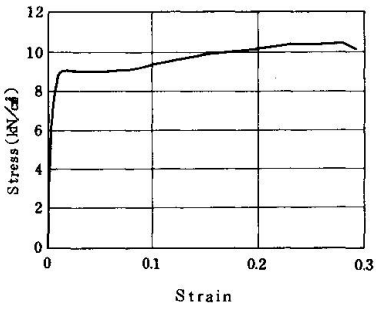


Fig. 9. Stress-strain relation

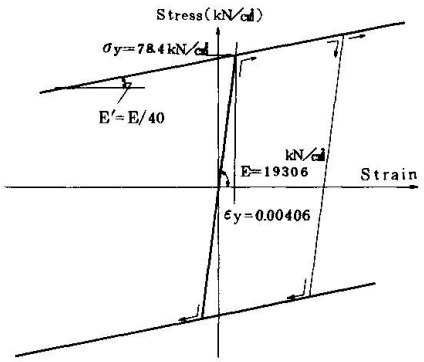


Fig. 10. Stress-strain relation (modeled)

## 4.3 Forming and contracting process

### 4.3.1 Forming process

An analysis for expressing the cold forming process, the bending moment (M) is given to the point Ⓠ as shown in Fig. 11 (processes O ⟶ A⟶B) until some of the layers yield . The desired shape is produced through residual deformation after the removal of the bending moment.

### 4.3.2 Expanding and contracting process

As an analysis for representing the expanding and contracting process, loading and unloading are repeated, the maximum load (P) being 117.6kN/m at which the average stress in the cross section becomes 7.84kN/cm$^2$ as shown by the processes B⟶C⟶D⟶E⟶F⇄G⇄H in Fig. 11.

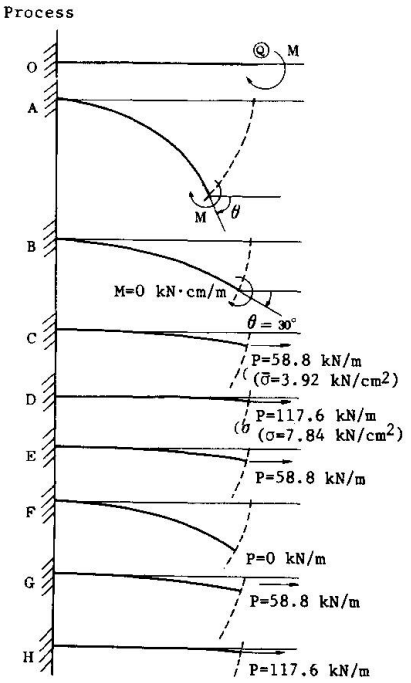


Fig. 11. Changes in deformation

## 4.4 Results of analysis

### 4.4.1 Relation between bending moment (M) and the angle of rotation (θ) (Fig. 12)

In the formation of a contraction joint with R of 20cm and θ of 30°, the desired shape can be produced by applying a bending moment of 42,111kN cm/m, rotating the point Ⓠ until θ becomes equal to 76.7° (process A), and removing the moment.

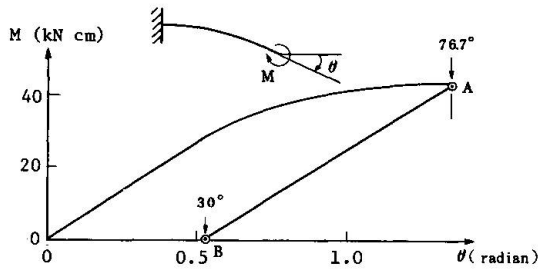


Fig. 12. M-θ relation

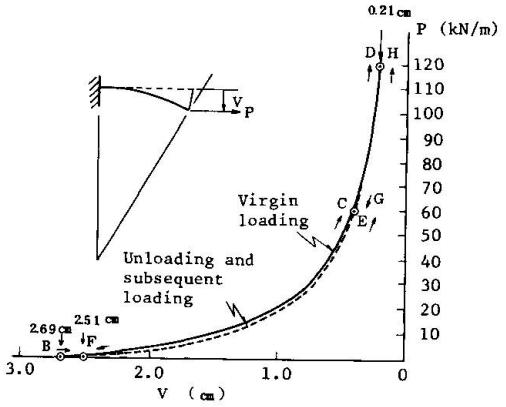


Fig. 13. P-V relation

4.4.2 Relation between load (P) and displacement (C) (Fig. 13)

When R is 20cm, the displacement V becomes 2.69cm at the end of forming (Process B). If virgin loading is done up to 118kN/m (process D), V becomes 0.21cm and the contraction joints extend nearly to a flat shape. The joints contract again if the load is removed. Even if the removal of load is completed (process F), however, V remains at 2.51cm and the contraction joints do not return to the originally formed shape. If the load is applied again, V becomes 0.21cm at the maximum load (process H). This V is the same as that obtained at the time of virgin loading (process D). Even if loading and unloading are repeated, the displacement in the respective processes does not vary.

4.4.3 Changes in stress and strain distributions at the fixed end (Fig. 14)

At the end of forming (process B), the residual stress and residual strain exist in the cross section. The strain is the largest under this condition but decreases as the load is removed. For the stress, the fiber stress reaches the yield level at P = 58.8kN/m (process C).

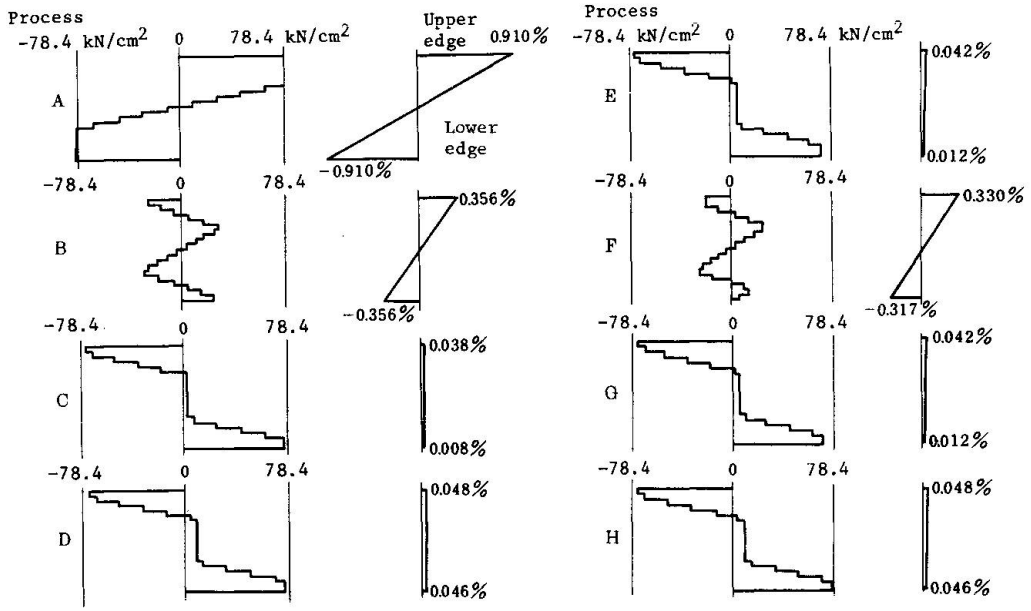


Fig. 14. Distribution of stress intensity at fixed end | Distribution of strain at fixed end | Distribution of stress intensity at fixed end | Distribution of strain at fixed end

4.4.4 Relation between fiber stress and strain at the fixed end (Fig. 15)

At the time of second and subsequent loading and unloading, the fiber stress and strain on surfaces change as the process proceeds from F through G to H and vice versa.

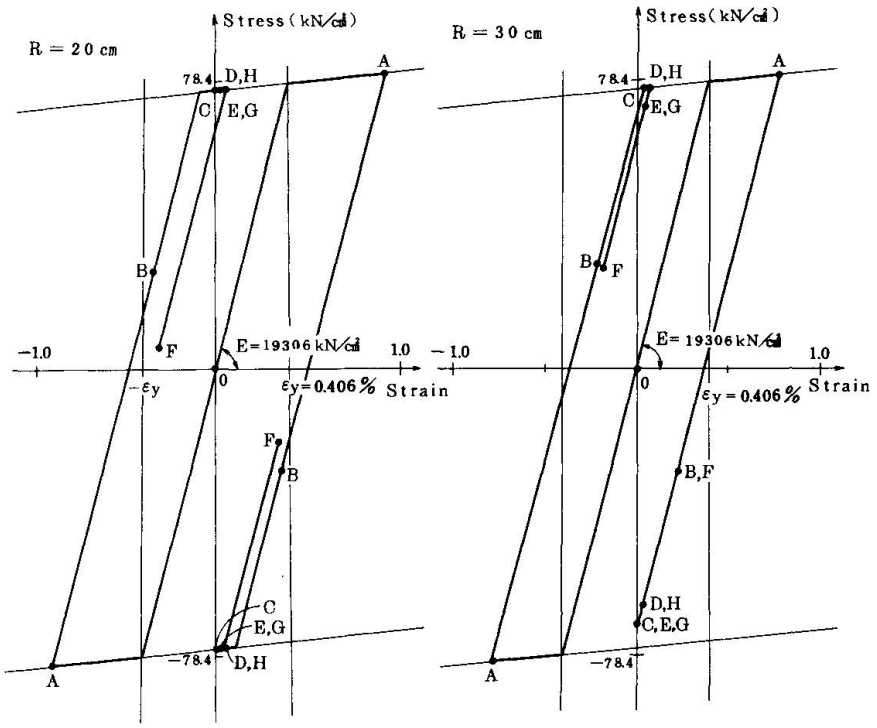


Fig. 15. Stress-strain relation of surface fiber stress

## 4.5 Study of structural safety

The study of the strain behavior of the contraction joint shows that the maximum strain is always below the yield strain and the maximum strain is caused under the no-load condition (process B or F). The study of stress behavior shows that the ratio of ultimate yield strength in the cross section to the integrated value of tensile stress in the cross section is higher than 4 as shown in Table 2, though there is such a case where yield occurs at the edge in the section when the maximum load is applied (process D or H). Based on these findings, it is said that the contraction joint is sufficiently high in structural safety.

Table 2

| Classification | Ultimate yield strength in cross section (kN/cm) a | Integrated value of tensile stress in cross section (kN/cm) b | Ratio a/b |
|---|---|---|---|
| R = 20cm | 11.76 | 2.94 | 4.0 |
| R = 30cm | 11.76 | 2.45 | 4.8 |

REFERENCE

1. FUJIMOTO, M. WADA, A. IWATA, M. Non-linear 3-dimensional analysis of Steel Frame Structure, A.I.J. No. 227, Jan. 1975.